Heliyon 10 (2024) e26868

Contents lists available at ScienceDirect

Heliyon

journal homepage: www.cell.com/heliyon

Research article

NANOPARTICLE-BASED formulation of dihydroartemisinin-lumefantrine duo-drugs: Preclinical Evaluation and enhanced antimalarial efficacy in a mouse model

Pesila Akeyo Odera [a,*], Geoffrey Otieno [a], Joab Otieno Onyango [a], James Jorum Owuor [a], Florence Anyango Oloo [a,d], Martin Ongas [c,d], Jeremiah Gathirwa [b], Bernhards Ogutu [c,d]

[a] School of Chemistry and Material Science, Technical University of Kenya, Nairobi Kenya
[b] Centre of Traditional Medicine and Drug Research, Kenya Medical Research Institute, Nairobi, Kenya
[c] Centre for Clinical Research, Kenya Medical Research Institute, Nairobi, Kenya
[d] Centre for Research in Therapeutic Sciences, Strathmore University Medical Centre, Nairobi, Kenya

ARTICLE INFO

Keywords:
Nanoformulation
Malaria
Lumefantrine
dihydroartemisinin
Antimalarials
Toxicity

ABSTRACT

Artemisinin-based combinations (ACTs) are World Health Organization-recommended treatment for malaria. Artemether (A) and lumefantrine (LUM) were the first co-formulated ACT and first-line treatment for malaria globally, artemether is dihydroartemisinin's (DHA's) prodrug. Artemisinins and LUM face low aqueous solubility while artemisinin has low bioavailability and short half-life thus requiring continuous dosage to maintain adequate therapeutic drug-plasma concentration. This study aimed at improving ACTs limitations by nano-formulating DHA-LUM using solid lipid nanoparticles (SLNs) as nanocarrier. SLNs were prepared by modified solvent extraction method based on water-in-oil-in-water double emulsion. Mean particle size, polydispersity index and zeta potential were 308.4 nm, 0.29 and −16.0 mV respectively. Nanoencapsulation efficiencies and drug loading of DHA and LUM were 93.9%, 33.7%, 11.9%, and 24.10% respectively. Nanoparticles were spherically shaped and drugs followed Kors-Peppas release model, steadily released for over 72 h. DHA-LUM-SLNs were 31% more efficacious than conventional oral doses in clearing *Plasmodium berghei* from infected Swiss albino mice.

1. Introduction

In 2021, an estimated 247 million malaria cases were reported globally from 84 malaria-endemic countries, showing an increase from 245 million recorded in the year 2020 with the most increase in African countries [1]. The sub-Saharan Africa Region recorded 234 million cases in the year 2021 representing almost 95% of the global malaria cases. The current malaria control tools are prompt diagnosis, chemotherapy, use of insecticide-treated nets and vaccination [2]. Artemisinin-based combinations therapies (ACTs) are the currently recommended treatments for uncomplicated malaria by the WHO [3] and parenteral artesunate as the first-line treatment for severe malaria [4] due to their efficacy, safety, and excellent tolerability [5]. However, the emergence of plasmodium resistance against artemisinins in the Greater Mekong sub-region [6] and other parts of Africa such as Uganda [7] and Rwanda [8] poses a global

* Corresponding author.
E-mail address: oderapesila1@gmail.com (P.A. Odera).

https://doi.org/10.1016/j.heliyon.2024.e26868
Received 22 November 2023; Received in revised form 19 February 2024; Accepted 21 February 2024
Available online 23 February 2024

threat to the gains made in fight against malaria. Dihydroartemisinin (DHA) as the active moiety of the artemisisnins [9] exhibits rapid parasite clearance and have been used in combination with a number of antimalarials such as amodiaquine, LUM, piperaquine, mefloquine and pyronaridine to save many lives [10]. The emergence of parasite resistance to artemisinins and lack of new antimalarial drugs highlight the need for designing new drug delivery systems to improve the pharmacokinetics and pharmacodynamics (PK/PD) of existing and new compounds to achieve better outcomes. The AL drug combination has low bioavailability, low aqueous solubility, non-specificity, with poor drug release profile [11]. The application of Nano-medicine in drug discovery can help in overcoming the pharmacokinetic and pharmacodynamics (PK/PD) shortfalls of the current antimalarial such as toxicity [12], low bioavailability [13] and non-specificity. There are a number of successful studies reported on antimalarial nanoformulations. Nano-emulsion of primaquine for instance improved its activity against *Plasmodium berghei* to 25% dose lower than conventional formulation and enhanced its uptake, oral bioavailability and accumulation in the liver [14]. Nano-formulated tafenoquine depicted a lower red blood cell hemolytic propencity [15]. Pharmacological activity of quinine was enhanced by its nano encapsulation [16] while microemulsion formulation of artemether showed a 1.5-fold increase in antimalarial activity [17]. Nano-formulated chloroquine functionalized with heparin showed an enhanced antimalarial efficacy against the chloroquine-sensitive (D6) strain of *P. falciparum* [18].

Heparin is classified as a glycosaminoglycan which targets the circumsporozoite protein in the sporozoite attachment to the hepatocytes during the earlier stage of malaria infection in the liver [19]. Glycosaminoglycan is a family of ubiquitous polysaccharide, some of whose members represent the most negatively charged natural polymers. Heparin, a glycosaminoglycan is an example of an inhibitory molecule with the ability to disrupt merozoite invasion [20] with very high affinity towards the parasitized red blood cells (*pRBCs)*. Heparin-like molecules have the ability to inhibit both sequestration and merozoite invasion hence reducing the parasitemia and malaria severity [21].

Lipid polymer based formulations enhance drug dissolution which improves their oral bioavailability [22]. Lipid-formulated drugs also have improved entrapment ability [23], improving their efficacy. The use of lipids with high levels of unsaturation improves the lymphatic uptake of lipid-based drug delivery systems, which prevents the hepatic first-pass metabolism of the drug [24]. This study nano-formulated DHA and LUM using solid lipid nanoparticles functionalized with heparin and tested their antimalarial efficacy through oral drug administration in an animal model. The *Plasmodium berghei* ANKA parasite was considered in the *in-vivo* study because it is a rodent malaria parasite that causes malaria infection in mice and it closely behaves like the *Plasmodium falciparum* parasites that cause malaria infection to human beings [25]. Most of the previous *in-vivo* antimalarial studies in mice have been conducted using *plasmodium berghei ANKA* parasites [26–28].

2. Methods

2.1. Materials

Chitosan low-viscous (CLV), Stearic Acid (SA), polyvinyl alcohol (PVA) with a molecular weight of 13,000–23,000, D-lactose monohydrate (DLM), ethyl acetate (EtOAc), acetic acid, and low molecular weight heparin sodium salt (>180 USP units/mg) were purchased from Sigma Aldrich in South Africa. Chemical reagents such as acetic acid and ethyl acetate were analytical grade. SA was used as the matrix; CVL acted as a mucoadhesive to improve the residence and intestinal nanoparticle circulation time. DLM acted as a binder to further reduce the nanoparticle size and acted as a potential agent for keeping up the osmotic balance in the blood. PVA was used as the main surfactant and emulsions stabilizer. Methanol-HPLC grades, dichloromethane, acetonitrile, ammonium formate, and formic acid were used as mobile phases in Liquid chromatography Mass Spectrometer (AGILENT TECHNOLOGIES 6410-TRIPLE QUAD LC/MS) that was accessed in a research laboratory at Centre. Pure standards (mefloquine, dihydroartemisinin, and lumefantrine) and deionized water obtained from a Thermo Scientific water deionizer, High-speed Centrifuge (EBA 200) and Sonicator (KERRY), Hot plate magnetic stirrer with maximum rotations per minute (rpm) of 6000, high-speed homogenizer with max rpm of 10,000 (Silverson L5-MA High speed homogenizer), bench top Buchi mini spray dryer (model BUCHI Mini Spray DryerB-290) accompanied with B-296 Dehumidifier, and Zeta-sizer (Malvern ZETASIZER NANO) were used for drug nano-formulation. All the reagents and excipients were used in drug reformulation as received. Scanning electron microscopy (SEM, Quanta FEG 250, FEI) was used to study the nano-formulated drug morphology. Fourier transform infrared (FTIR) (JASCO 4700 ATR-FT/IR) was accessed from the School of Pharmacy & Health Sciences at the Unit. Sodium lauryl sulfate (SLS), acetate buffer, pH meter, dialysis membrane bags (MWCO: 12–14 kDa) were used for the drug release kinetic studies.

2.2. Preparation of solid lipid nanoparticles

Nano-particles were prepared using a single emulsion solvent evaporation technique. Preparation method used by Omwoyo et al. [24] was adopted with slight modifications. Organic phase of formulation was prepared by dissolving 50 mg of stearic acid in 10 mL ethyl acetate. 10 mg and 60 mg of dihydroartemisinin and lumefantrine were added to organic phase respectively. Aqueous phase was made up of a mixture of 10 mL, 2% (w/v) PVA, 1 ml, 1% (w/v) heparin, 5 mL, 5% (w/v) DLM, and 5 mL, 0.3% (w/v). Resultant oil in water emulsion was emulsified for 10–15 min by high-speed homogenization with speeds varied between 8000 and 10,000 rpm. High-speed homogenization process provides necessary energy for a nano-formulation process that uses a solvent evaporation technique [25]. During homogenization by the solvent extraction process, proper particle dispersion takes place forming smaller-sized nano-particles [26]. Oil-water (O/W) emulsion obtained was fed directly into a benchtop Buchi mini-spray dryer and spray-dried at 90 °C–120 °C and atomizing pressure varied between 4 and 7 bars. Resultant nanoparticles were characterized for particle charges,

particle size, encapsulation efficiency, polydispersity index, morphology, structure, drug loading (DL%) antimalarial activity, and cytotoxicity. Two factorial experimental design was used to optimize desirable nano-formulation conditions in terms of matrix concentration, homogenization speed, time, surfactant types and concentrations.

2.2.1. Characterization of the nanoparticles

I. Particle size analysis

The Malvern Zetasizer Nano computerized system was used to measure nanoparticle size, zeta potential, and polydispersity index. 2 mg of the samples were suspended in distilled water, vortexed, and sonicated, and transferred to current-conducting cuvettes for analysis. The measurements were conducted at 25 °C, at an angle of 173°

II. Storage stability studies of DHA-LUM Solid Lipid Nano-particles

The nano-formulated drug samples were evaluated for stability following the International Conference on Harmonisation (ICH) guidelines Q1 (R2) [29]. The nano-formulation process involved an upscaling of the oil/water emulsion production process in order to get enough nano-particles for the stability study. The samples were stored for four months at 25 °C and 4 °C, and characterized periodically based on size, zeta potential, and polydispersity index. 1 mg drug samples were suspended in distilled water, vortexed (a Cole-Parmer vortex (VM3), and sonicated (KERRY).

III. Morphological examination

Nano-formulated samples' morphology and topography were analyzed using SEM (SEM, Quanta FEG 250, FEI), with gold coating applied before analysis to reduce heat effects and the particles SEM images captured.

IV *In-vitro* drug release studies

A study on nano-formulated drug release kinetics was conducted by using Gao et al. (2013) [30] modified method. 20 mg of drug samples were dissolved in 2 ml, of 2% (w/v) Sodium lauryl sulfate (SLS) in 0.1 M acetate buffer (pH 4.5) solution and transferred to dialysis membrane bags (MWCO: 12–14 kDa). The bags were then transferred to a beaker with 100 ml of dissolution solution (0.1 M acetate buffer (pH 4.5) solution). The beakers incubated at 37 °C and 100 rotations per minute, and the solutions were periodically collected for LC/MS analysis.

V. Encapsulation efficiency and drug loading

Nano formulated drugs were suspended in de-ionized water, vortexed, and ultracentrifuged (SL 40R centrifuge) for 20 min at 3000 rpm at 4 °C. The supernatant was diluted for LC/MS analysis, and drug loading and encapsulation efficiency were calculated using formulas 1 and 2.

$$\%\text{Drug Loading} = \frac{100(Drug\ in\ precipitate)}{Drug\ in\ precipitate + Added\ excipients**} \quad (1)$$

$$\%\text{Encapsulation Efficiency} = \frac{100(Drug\ in\ precipitate*)}{Total\ added\ drug} \quad (2)$$

*Drug in precipitate = Total drug added-Free drug after ultracentrifugation.

***Added excipients = Lipids + Surfactants + other ingredients (e.g., in drug Nano formulation).

High drug loading capacity was achieved by having a sufficiently high soluble drug in the lipid melt. Drug solubility in the lipid melt is heightened by adding solubilizers and the presence of mono-and diglycerides in the lipid matrix [31].

VI. Fourier Transform Infrared (FTIR) Spectroscopy

FTIR spectral analysis was used to determine functional groups of compounds on drug surfaces. A method developed by Thiruvengadam and Bansod, (2020) was used to prepare and analyze nanoparticles [32]. 5 mg of the samples were spread between KBr plates, and the spectrometer scanned the 4400-400 cm−1 wavenumber region to obtain spectral readings.

VII. Evaluation of antimalarial efficacy

Ethical approval

Swiss Albino mice were selected as the subjects for the antimalarial efficacy, acute, and sub-acute toxicity studies. Before initiating these investigations, the research protocol received ethical approval from Kenya Medical Research Institute's (KEMRI) Animal Care and Use Committee (ACUC) and the Scientific & Ethical Review Unit (SERU). The study was granted certificate number KEMRI/SERU/

Table 4
Chemosuppression efficiency and mice survival rates.

S. No	Drug	% Chemosuppression efficiency Average ± StDev	Mice Survival time (days)
1	Nano-formulated DHA-LUM with heparin	88.77 ± 8.55	>60.00
2	Free drugs: DHA-LUM with heparin	57.15 ± 12.69	12.00 ± 0.02
3	Nano-formulated DHA-LUM without heparin	79.34 ± 15.53	>60.00
4	Free drugs: DHA-LUM without heparin	35.27 ± 15.15	11.00 ± 0.10
5	Empty nanoparticle without heparin	31.63 ± 12.99	10.00 ± 0.05
6	Empty nanoparticle with heparin	59.15 ± 8.92	14.00 ± 0.03
7	Negative control	0.00 ± 0.00	12.00 ± 0.01

CTMDR/069/3833.

Animal studies followed Organization for Economic Co-operation and Development (OECD) guidelines, ensuring mice's well-being and results validity. They were taken through seven-day acclimatization period before experiments began.

In a 4-day *in vivo* suppressive test, 5 male Swiss albino mice were used per group and infected intraperitoneally with blood containing parasitized 2×10^6 *P. berghei* ANKA red blood cells contained in 0.2 mL inoculums on day zero and orally treated with various doses of DHA-LUM SLNs 2 h post-infection. The *Plasmodium berghei ANKA* parasite was the parasite of choice because it is a rodent malaria parasite that causes malaria infection in mice and they closely behave like the *Plasmodium falciparum* parasites that cause malaria infection to human beings. The negative control group received the vehicle used to suspend samples. Drug administration was repeated 24, 48, and 72 h post-infection. Blood smears were taken by making a thin film from a tail snip of each mouse on 96 h post-infection, and fixed in methanol and stained with 10% Giemsa for 20 min. The percentage of parasite reduction was calculated using the formula [(A-B)/A]*100, where A represented the mean parasitaemia in the negative control group and B represented the parasitaemia in the test group as described by Tona & Mesia (2001) [33]. The percentage of chemo suppression efficiency presented in Table 4 represents the percentage of parasite reduction by the duo nano-formulated drugs. The mice were monitored for 60 days, and survival rates were calculated.

VIII. Toxicity study on the duo nano-formulated drugs

2.2.2. Experimental animals

The KEMRI animal house provided mice aged 18.00 ± 2.00 g each, maintained under standard conditions (temperature 25 ± 2 °C, 12-h light-dark cycle, and relative humidity of 75 ± 5%), fed on mice pellets and tap water *ad libitum*.

Preparation of the duo nano-formulated drugs.

Nano-formulated drugs were dissolved in distilled water and administered to animals for toxicological evaluations, with 0.2 ml of distilled water administered as the negative control.

2.2.3. Experimental design

i. Acute toxicity experiment

Male Swiss albino mice were considered for the study and a total of five (5) mice per each study group were used. The study involved mice divided into four groups, each with different drug concentrations (1,000 mg/kg b.w dose, 2,000 mg/kg b.w dose and 5,000 mg/kg b.w). The mice were starved overnight and weights recorded prior to dosing. Mice from different groups were placed in different cages and carefully labelled. Plastic box cages with sawdust at the base with drinking water and feed provisions were used. The control group received 0.2 ml of distilled water, while the test group received single doses of the above concentrations. Mice were monitored daily for 14 days for any sign of toxicity, and their body weights recorded. On day 14, the mice were starved and sacrificed, and their internal organs, kidneys, liver, and spleen surgically removed and examined for toxicity.

ii. Sub-acute toxicity experiment

Twelve male Swiss albino mice were divided into four groups, each with varying drug concentrations (154.8, 309.6 and 464.6 mg/kg b.w). The drug concentrations were calculated using the probit log analysis with 154.8 mg/kg b.w considered as the therapeutic concentration, 309.6 mg/kg b.w and 464.6 mg/kg b.w represented medium and high concentrations respectively [34]. Mice were starved overnight and their weights recorded before dosing. The control group received 0.2 ml of distilled water, while the test group received single doses of 154.8 mg/kg, 309.6 mg/kg, and 464.6 mg/kg daily for 28 days. Mice were starved on the eve of the 28th day, euthanized using carbon-dioxide gas as a safe and standard way of sacrificing laboratory mice, and necropsied, and their organs were examined for toxicity [35]. The spleen, kidney and liver of the treated mice were compared to those of the negative control mice by comparing the organ appearances, size, colour and consistency.

a Histopathological studies

Organs were surgically removed, weighed, and stored in formalin for histopathological examination. Relative weight was

Table 1
The particle sizes, zeta potential and polydispersity index values of empty and drug loaded nanoparticles.

Sample	Particle size (nm)	Zeta potential (mV)	Polydispersity index
Empty nanoparticle without heparin	387.8 ± 19.9	39.2 ± 2.5	0.49 ± 0.07
Empty nanoparticle with heparin	218.0 ± 12.0	−26.9 ± 10.0	0.20 ± 0.05
DHA-LUM SLNs drug functionalized with heparin	308.4 ± 3.8	−16.0 ± 1.3	0.29 ± 0.02

Table 2
Nano-particle size and zeta potential variations with changes in temperature.

Days	Zeta potential (mV)		Particle Size (nm)	
	at 4 °C	at 25 °C	at 4 °C	at 25 °C
0	−23.4	−23.4	355.1	355.1
5	−19.5	−23.6	361.3	406.4
15	−22	−26.2	363.0	408.5
30	−22.2	−27.1	364.2	410.4
60	−22.5	−27.4	365.3	410.5
90	−23.1	−34.1	369.5	417.3
120	−23.4	−34.3	370.5	418.2

calculated using mice's body weights by adopting the formula described by Tizifa et al. (2018) [2]: (organ weight/body weight on the day they were sacrificed) *100. Histopathological examination was performed using a standard laboratory procedures [36].

b. Biochemistry tests

Blood samples were centrifuged without any additive at 4000 rpm for 10 min at 4 °C and stored at 4C for further analysis, to separate serum from other blood cells, and biochemical analysis done using an Erba XL-180 Fully Automated Chemistry Analyzer. Key indicators included creatinine (Cr), urea, Bilirubin Direct (DBIL), aspartate aminotransferase (AST), and alanine aminotransferase (ALT).

c Hematological index

Blood samples were analyzed using EDTA-K_2 tubes, and hematological parameters were determined using standard biochemistry tests [37]. Hematological index analysis was done using a Hematology analyzer (Sysmex XS 500i). Hematological index indicators were platelet count (PLT), mean corpuscular hemoglobin concentration (MCHC), mean corpuscular hemoglobin (MCH), mean corpuscular volume (MCV), hemoglobin (HGB), red blood cells (RBCs), and white blood cells (WBCs).

2.2.4. Statistical analysis

The study data in this work were expressed as mean and standard deviations (Mean ± SD) and the data were statistically analyzed using one-way analysis of variance (ANOVA). A $p<0.05$ values considered statistically significant. The curves and graphs were drawn using Origin 2018 64 Bit software.

3. Results and discussion

3.1. Particle size analysis

Table 1 summarizes SLN particle sizes, zeta-potential, and polydispersity index. Empty nanoparticles with heparin have lower particle size than the drug loaded nanoparticles. The study successfully achieved a targeted particle size of $x \leq 500$ nm for the duo nano-formulated drugs, allowing their swift movement through the gastro-intestinal tract.

3.2. SLN stability studies

Table 2 summarizes stability of SLN nano-formulated DHA-LUM-duo formulation with heparin; storage for 120 days did not significantly affect drug size, charges, or homogeneity.

The stability of nano-formulated drugs stored at 4 °C and 25 °C as represented in Table 2 was enhanced due to the removal of water and solvents during spray drying, resulting in a stable sample, a finding consistent with previous studies [38].Therefore, kinetic energy that could have been increased by constant motion of particles in an emulsion was eliminated in the dry powdered samples. The stability of the dry powdered sample therefore increased even at an elevated temperature.

Table 3
The coefficient of determination (R^2) values of the curves produced by DHA and LUM mathematical models.

Serial numbers	Drug release kinetic model	DHA R^2 value	LUM R^2 value
1.	Kors-peppas	0.9823	0.9534
2.	Higuchi	0.9346	0.9101
3.	First order	0.8709	0.7684
4.	Hixson	0.8525	0.7503
5.	Zero order	0.8137	0.7138

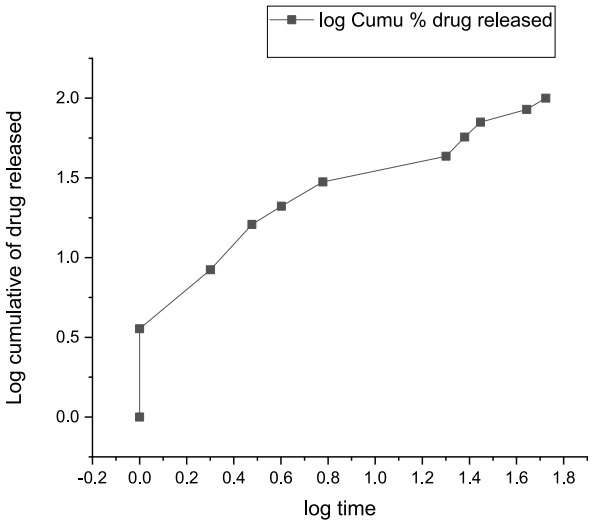

Fig. 1. Kors Peppas mathematical model followed by DHA drug in the duo nano-formulated samples.

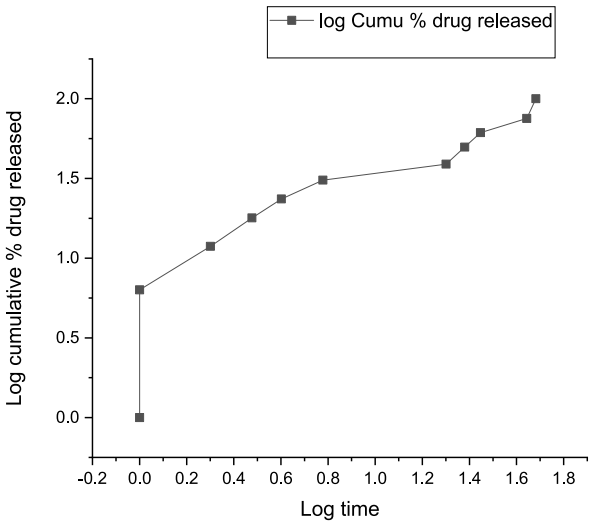

Fig. 2. Kors Peppas mathematical model followed by lumefantrine drug in the duo nano-formulated samples.

3.3. In-vitro drug release study results

Table 3 displays R^2 values for drug release data in various pharmaceutical models, while Figs. 1 and 2 summarize the results of the periodic drug release study [39].

Haghiralsadat et al. (2018) reported that the best-fitted model with the release data is evaluated by the coefficient of determination (R^2) [40]. Table 3 shows R^2 values obtained by fitting DHA and LUM drug release data into drug mathematical models. Results in

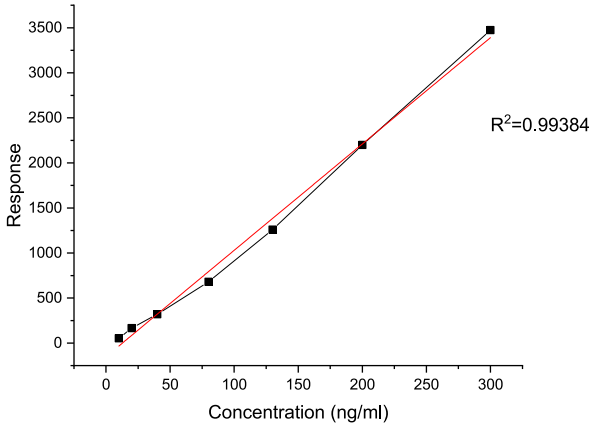

Fig. 3. Calibration curve for DHA free drug.

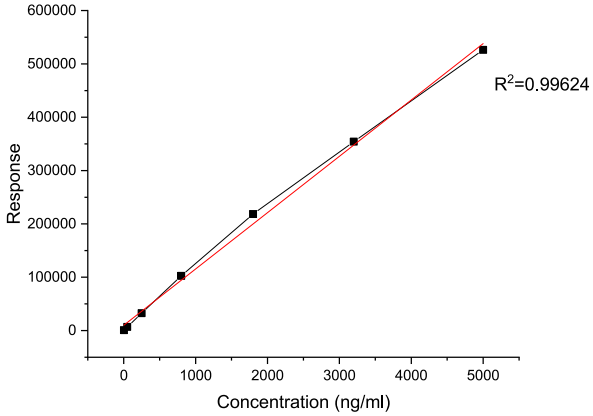

Fig. 4. calibration curve for LUM free drug.

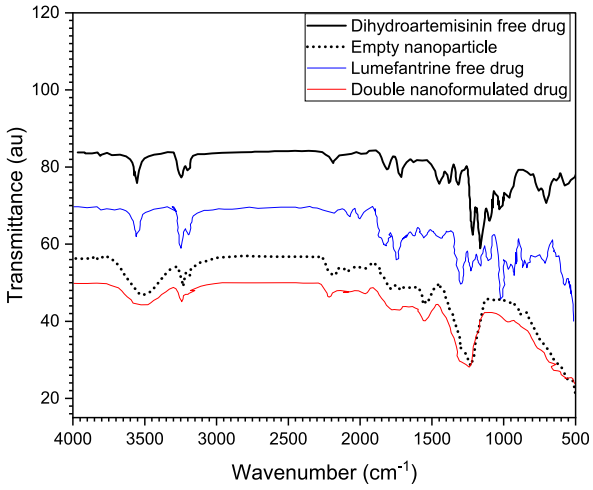

Fig. 5. FTIR overlay spectra for empty nanoparticles, free drugs (DHA & LUM) and duo nano-formulated drugs.

Figs. 1 and 2 show that they followed Korsmeyer-Peppas release model. Korsmeyer-Peppas and Higuchi models successfully explained release of nano-liposome formulated drugs [41]. They are non-linear regression models, used in interpreting non-linear diffusion profiles. A study conducted by Jain and Jain, 2016 [42] showed that the drug transport profiles taking place through regenerated

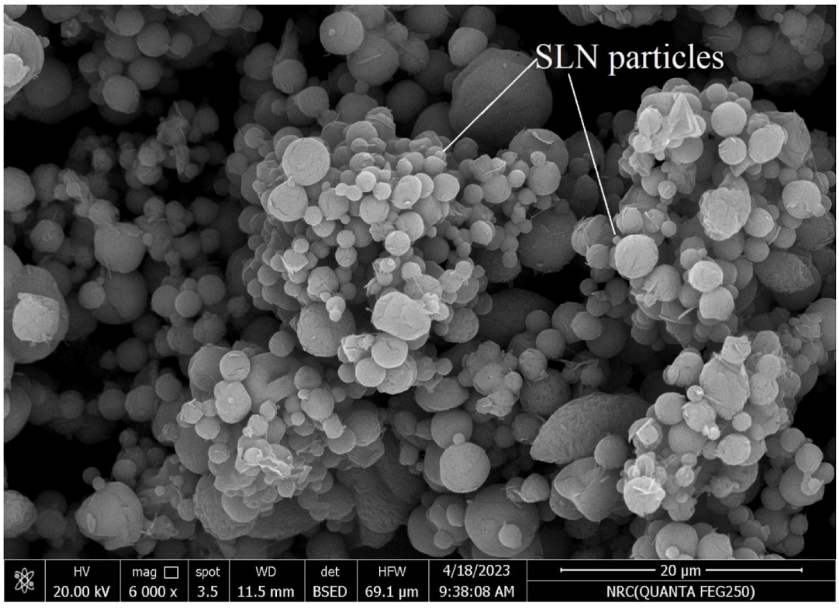

Fig. 6. Scanning electron microscopy images of the duo nano-formulated solid lipid nanoparticle samples.

cellulose barriers deviates from linearity [43]. Korsmeyer-Peppas model also shows release of drugs from polymeric systems while Higuchi model explains drug released through diffusion mechanism [39,43]. These were demonstrated in our conducted experiment, as represented in Table 3, Figs. 1 and 2, free drugs moved from the visking tubing bags to the dissolution solution through diffusion process. DHA and LUM free drugs released from the nano formulated drugs exhibited a burst drug release in the first 6 h followed by a controlled release of the drugs. The curve flattened between the 24th-72nd hour indicating an equilibrium point between drug concentrations and dissolution solution.

Duo nano-formulated drugs show encapsulation efficiency of 93.92 ± 0.47% and 33.65 ± 1.58%, with loading capacities of 11.87 ± 0.04% and 22.38 ± 0.76%, respectively. The calibration curves of DHA and LUM are shown in Figs. 3 and 4.

3.4. FTIR results

Fig. 5 displays FTIR overlay spectra of empty nanoparticles, free drugs, and nano-formulated drugs. FTIR bands of empty nanoparticles and nano-formulated drugs showed almost similar absorption peaks.

The FTIR overlay spectra represented the functional groups of compounds in drug excipients and compounds. The wavenumbers exhibited in both empty and duo nano-formulated drug samples were: 3308.29 cm^{-1} exhibiting the presence of –OH in the structure of polyvinyl alcohol, 2914.88 cm^{-1} representing strong band, associated with C–H in polyvinyl alcohol [44] and aliphatic C–H in stearic acid, 2853.17 cm^{-1} represented aliphatic C–H vibration in stearic acid [45], 1416.46 cm^{-1} represented C–O bending peak in stearic acid, 1372.10 cm^{-1} represented CH_3 symmetrical deformations in chitosan [46], and absorption peaks exhibited at around 1248.68 cm^{-1} represented the bending vibration of hydroxyls that exist in chitosan molecules [47] as reported in other studies. Additionally, more pronounced peaks evidenced in the two free drugs were absent in nano-formulated drugs. LUM free drug exhibited pronounced absorption peaks at O–H aromatic stretching at 3402.70 cm^{-1}, C–O stretching at 1139.22 cm^{-1} and C═C aromatic stretching at 1575.43 cm^{-1}. OH-absorption peak that was more pronounced in DHA free drug samples at wavelength number 3732 cm^{-1} was absent in the nano-formulated drug samples, indicating successful encapsulation of the duo antimalarial drugs [48,49]. This could be due to the use of D-Lactose Monohydrate as a structure binder, reducing the number of pronounced peaks in the nano-formulated drugs [50].

3.5. Drug loading and encapsulation efficiencies

Nanoencapsulation efficiencies and drug loading of DHA and LUM were 93.9%, 33.7%, 11.9%, and 24.10% respectively. Drug loading capacities and nanoencapsulation efficiencies are key nanoparticle characterization parameters. Solid lipid nanoparticle is a drug strategy entailing drug encapsulation during nanoparticle formation [51] and an example of drug co-loading strategy. Drug loading values achieved using co-loading strategies range between 18.5 and 100%, particle sizes range from 29 to 400 nm [52]. Studies have reported drug loading and encapsulation efficiencies of 12.03% and 97% for Ketoprofen and 13.9% and 62.3% for dihydroartemisinin [51,52] and 13.9% and 62.3% for dihydroartemisinin [53]. Drug loading capacities of 20%, 5%, and 20–25% for coenzyme Q10, retinol, and cyclosporine respectively have been reported in literature [54,53]. The DHA-LUM duo nano-formulated drug in this experiment showed comparable drug loading capacities. Factors affecting drug loading and incorporation include supercooled melts, lipid material polymorphism, solid lipid matrix structure, and drug solubility.

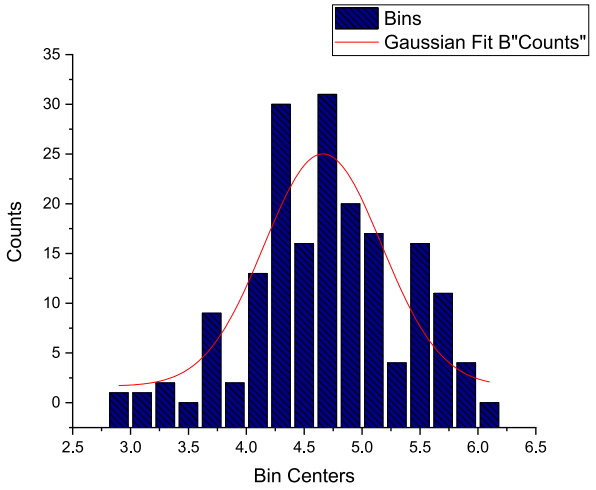

Fig. 7. Histogram showing particle size distribution of the duo nano-formulated solid lipid nanoparticle samples.

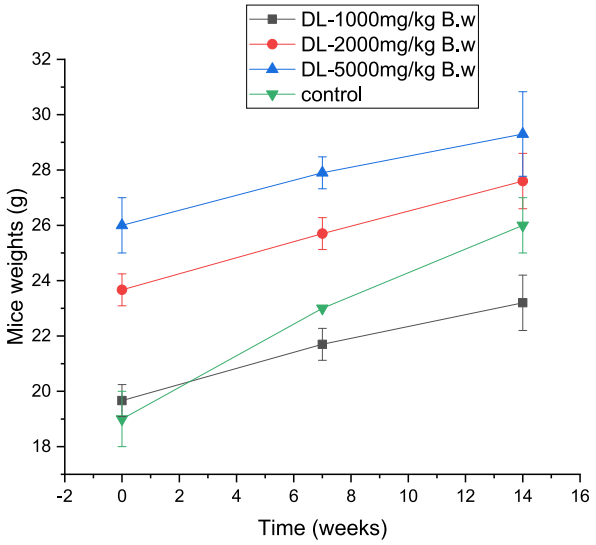

Fig. 8. line graph showing weight variations of mice during acute toxicity study.

3.6. SLN Morphological results

Fig. 6 displays SEM images of DHA-LUM duo nano-formulated drugs, showing spherical, smooth, and fibrous surfaces, processed using image j software. A few SLN particles have been marked and labelled in Fig. 6. The particle sizes were well distributed as processed and represented by a histogram in Fig. 7.

Fig. 6 represented images of DHA-LUM duo nano-formulated drugs from the scanning electron microscope. Spherical SEM images with smooth and fibrous surfaces are associated with the solid lipid nano-particle spherical shapes [48] were formed. Fibrous surfaces indicating the inclusion of chitosan for improved muco-adhesiveness, biocompatibility, and bio-degradability [49]. The image showed slightly homogenous granulated particles interlinked to each other with pores existing between them. Literature has reported that particles with granulated, homogenous and porous structures are important in biological applications [55]. The SEM images were further processed using image j software and their homogenous distribution is represented in histogram (Fig. 7).

3.7. Antimalarial efficacy

Table 4 shows the anti-plasmodium efficacy results as was executed using *in vivo* experiments in Swiss albino mice. Different test groups considered for the *in-vivo* experiments; empty nanoparticles examined against plasmodium parasites to find out whether excipients used in drug-reformulation had antimalarial activity or not. Empty nano-particles without heparin and test group treated with

Table 5
Data analysis parameters of relative weights, organ hematological, and biochemical parameters.

Parameters	Normal control	Low concentration (154.8 mg/kg)	Medium concentration (309.6 mg/kg)	High concentration (464.6 mg/kg)	P-Value
Organ relative weights					
Spleen	0.53 ± 0.06	0.35 ± 0.02	0.46 ± 0.04	0.50 ± 0.03	0.05
Kidney	2.44 ± 0.37	2.33 ± 0.16	2.31 ± 0.04	2.52 ± 0.13	0.88
Liver	6.14 ± 0.62	7.61 ± 0.67	7.21 ± 0.25	6.89 ± 0.40	0.30
Hematological parameters					
White blood cells ($x10^3$/u/L)	4.39	5.22	4.78	4.11	0.56
Red blood cells ($x10^6$/u/L)	10.69	9.99	10.96	11.01	0.49
HGB (g/dL)	15.90	14.73	15.13	15.90	0.66
HCT (%)	54.73	52.03	54.20	52.13	0.54
Mean Corpuscular Volume (fL)	49.30	52.33	49.40	49.23	0.32
Mean Corpuscular Hemoglobin (pg	14.87	14.77	14.03	14.43	0.01
Mean Corpuscular Hemoglobin Con	30.17	29.80	28.43	28.23	0.11
RDW-CV (fL)	26.33	23.03	25.87	26.40	0.09
Platelets ($x10^3$/Ul)	1145.00	571	833.30	852.70	0.02
Biochemical parameters					
ALT	52.40 ± 2.38	53.77 ± 2.23	54.23 ± 1.24	56.53 ± 2.62	0.62
AST	179.63 ± 3.26	180.57 ± 1.52	180.80 ± 1.35	181.33 ± 1.24	0.94
Bilirubin Direct (mg/dl)	0.05 ± 0.01	0.07 ± 0.01	0.07 ± 0.01	0.07 ± 0.02	0.24
Urea	50.73 ± 1.52	51.10 ± 1.69	56.30 ± 0.17	50.93 ± 1.87	0.08
Creatinine	0.50 ± 0.02	0.51 ± 0.03	0.50 ± 0.03	0.46 ± 0.02	0.55

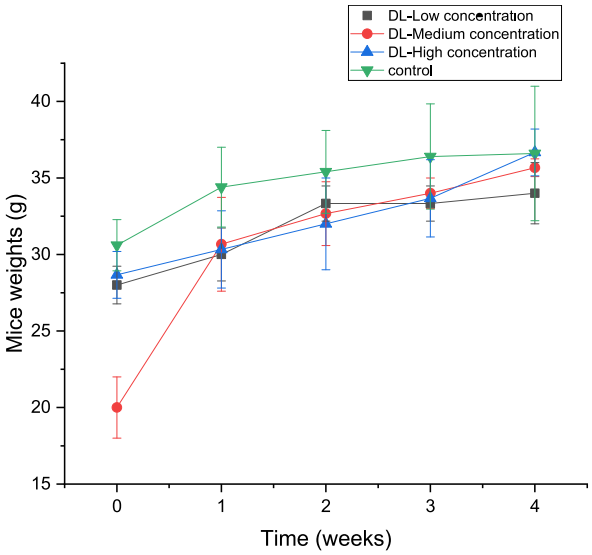

Fig. 9. line graph showing weight variations of mice during the 28 days sub-acute toxicity study (Low = 154.8, medium = 309.6, high = 464.6 mg/kg).

control showed very low chemosuppression. However, empty nanoparticles with heparin showed higher chemosuppression efficiency than empty nano-particles without heparin.

The examination of anti-plasmodium efficacy was executed using *in-vivo* experiments in Swiss albino mice (Table 4). *In-vivo* experiments on Swiss albino mice showed that empty nanoparticles with heparin showed higher chemosuppression efficiency than those without heparin. This could be attributed to the fact that heparin, a glycosaminoglycan with antimalarial activity, was found to be effective against plasmodium-infected red blood cells as reported in other studies [55,56]. Duo nano-formulated drugs showed higher parasite chemo suppression efficiency, with mice surviving over sixty days without toxicity signs as shown in Table 4. Mice treated with free drugs exhibited signs of toxicity like rough hairs and diarrhea; which could have also been attributed to the high parasitemia levels. The nano-formulated drugs showed a significant chemosuppression ($p<0.05$) compared to the free drugs. These findings are consistent with previous studies on dihydroartemisinin [53] and primaquine [50] nano-formulated drugs.

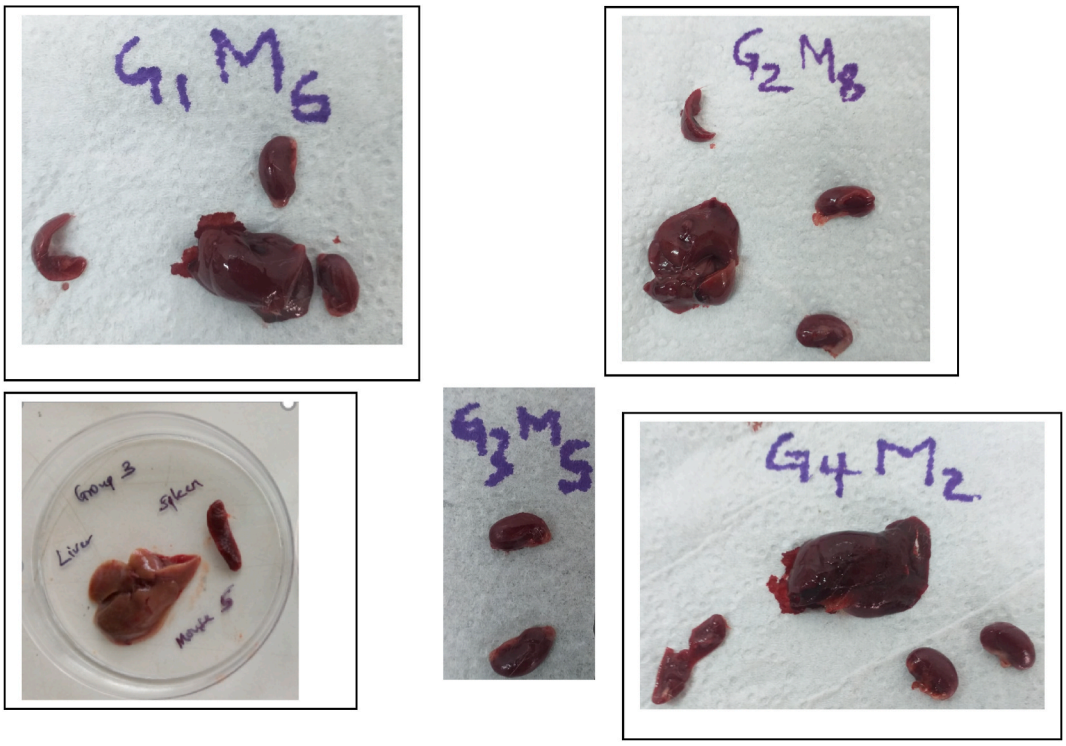

Fig. 10. Representative Histopathological study organs (spleen, liver and kidney) for the sub-acute toxicity study.

3.8. Toxicity study results

3.8.1. Acute toxicity study

During the acute toxicity study, no toxic symptoms were observed in mice, including rough hair, depression, diarrhea, and restlessness. Major body tissues, liver, spleen, and kidney showed no abnormalities. No mortalities were recorded, and mice showed normal weight increase as illustrated by Fig. 8, indicating no adverse effects from drugs.

3.8.2. Sub-acute toxicity study

The sub-acute toxicity study found no visible signs of toxicity or mortalities in mice treated with the duo nano-formulated drugs. The mice's organ weights, biochemical tests, and hematological parameters did not show significant differences compared to the control group ($p > 0.05$) as represented in Table 5. However, MCH and platelet count showed significant differences ($p<0.05$) as shown in Table 5. The mice did not show significant variations in their weights during the 28-day sub-acute toxicity study as shown in Fig. 9. The histopathological organs of treated mice and the control mice did not show any significant difference as shown in Fig. 10.

Safety studies on drug products are conducted by performing sub-acute and acute toxicity tests in laboratory animals such as non-human primates and rodents [57]. The acute and sub-acute oral toxicity of the duo nano-formulated drugs in Swiss albino mice were investigated in this study. The acute toxicity study observed effects for 14 days after a single dose, while the sub-acute toxicity study observed effects over a prolonged period with recurrent administration [58]. The drug doses used in the acute toxicity study were 1000 mg/kg, 2000 mg/kg, and 5000 mg/kg representing low, medium and high doses respectively. The lethal dose $(LD)_{50}$ of duo nano-formulated drug was therefore >5000 mg/kg because no mortalities or toxicity signs were recorded during the whole monitoring period. Substances with an $LD_{50} > 2000$ mg/kg are considered as safe according to Globally Harmonized System (GHS) of classification and labelling of chemicals [59]. Other therapeutic plant extracts used in other studies found to have $LD_{50} > 2000$ mg/kg have been categorized as reasonably safe as per the GHS criterion [60]. The clinical symptom results did not show any change in mice posture, mucosal color, and general behavioral change. The sub-acute toxicity results did not allude to any form of drug toxicity to the Swiss albino mice.

4. Conclusion and study limitations

The nano-formulated AL was found to be stable, safe and efficacious in parasitemia suppression and there is need to further optimization this duo contamination for further development. However, the study had a few limitations which majorly included the inability of undertaking full nano-formulated drug characterization due to lack of some key research equipment like differential scanning colorimetry, thermal gravimetric analysis equipment, and the inability to conduct *in-vitro* antimalarial bioassay. The

histopathological study was not fully concluded due to greater costs involved in acquiring the services of pathologist to interpret the microtomy microscopic slides.

6. Disclosure

The authors declare no conflict of interest in this research study.

Data availability

Sharing research data helps other researchers evaluate your findings, build on your work and to increase trust in your article. We encourage all our authors to make as much of their data publicly available as reasonably possible. Please note that your response to the following questions regarding the public data availability and the reasons for potentially not making data available will be available alongside your article upon publication.

Data included in article/supp. material/referenced in article.

CRediT authorship contribution statement

Pesila Akeyo Odera: Writing – review & editing, Writing – original draft, Project administration, Methodology, Funding acquisition, Formal analysis, Data curation, Conceptualization. **Geoffrey Otieno:** Writing – review & editing, Validation, Supervision. **Joab Otieno Onyango:** Writing – review & editing, Supervision, Formal analysis, Data curation. **James Jorum Owuor:** Writing – original draft, Methodology, Data curation. **Florence Anyango Oloo:** Formal analysis, Data curation. **Martin Ongas:** Methodology, Formal analysis, Data curation. **Jeremiah Gathirwa:** Writing – original draft, Resources, Project administration, Conceptualization. **Bernhards Ogutu:** Writing – review & editing, Resources, Funding acquisition, Conceptualization.

Declaration of competing interest

The authors declare the following financial interests/personal relationships which may be considered as potential competing interests:Dr. Bernards Ogutu reports financial support, administrative support, equipment, drugs, or supplies, statistical analysis, and travel were provided by the National Research Fund, Kenya. NONE has a patent NONE pending to NONE. NONE If there are other authors, they declare that they have no known competing financial interests or personal relationships that could have appeared to influence the work reported in this paper.

Acknowledgments

The authors of this study sincerely thank the National Research Fund (NRF) Kenya for funding this work. NRF did not participate in collection, analysis and interpretation of data. They however approved publication of the research findings. The authors would also wish to express gratitude to the Kenya Medical Research Institute (KEMRI), The Centre for Research in Therapeutic Sciences (CREATES), The Technical University of Kenya (TUK),and the Institute of Primate Research (IPR) for availing essential facilities to conduct the research study and creating a conducive environment for the research work.

Appendix A. Supplementary data

Supplementary data to this article can be found online at https://doi.org/10.1016/j.heliyon.2024.e26868.

References

[1] World Malaria Report 2022, 2022.
[2] T.A. Tizifa, A.N. Kabaghe, R.S. McCann, H. van den Berg, M. Van Vugt, K.S. Phiri, Prevention efforts for malaria, Curr. Trop. Med. Reports 5 (1) (2018) 41–50, https://doi.org/10.1007/s40475-018-0133-y.
[3] T.M.J. Maugueret, S.L. Walker, Rapid detection of Obesumbacterium proteus from yeast and wort using polymerase chain reaction, Lett. Appl. Microbiol. 35 (4) (2002) 281–284, https://doi.org/10.1046/j.1472-765X.2002.01179.x.
[4] A.M. Dondorp, et al., Artesunate versus quinine in the treatment of severe falciparum malaria in African children (AQUAMAT): an open-label, randomised trial, Lancet 376 (9753) (2010) 1647–1657, https://doi.org/10.1016/S0140-6736(10)61924-1.
[5] R.J. Maude, et al., The last man standing is the most resistant: eliminating artemisinin-resistant malaria in Cambodia, Malar. J. 8 (1) (2009) 1–7, https://doi.org/10.1186/1475-2875-8-31.
[6] M. Imwong, et al., The spread of artemisinin-resistant Plasmodium falciparum in the Greater Mekong subregion: a molecular epidemiology observational study, Lancet Infect. Dis. 17 (5) (2017) 491–497, https://doi.org/10.1016/S1473-3099(17)30048-8.
[7] H.S. Rates, et al., Artemisinin-Resistant plasmodium falciparum with high survival rates, Uganda, 2014-2016, Emerg. Infect. Dis. 24 (4) (2018) 718–726.
[8] A. Uwimana, et al., Association of Plasmodium falciparum kelch 13 R561H genotypes with delayed parasite clearance in Rwanda: an open-label, single-arm, multicentre, therapeutic efficacy study, Lancet Infect. Dis. 21 (8) (2021) 1120–1128, https://doi.org/10.1016/S1473-3099(21)00142-0.
[9] R. Yu, G. Jin, M. Fujimoto, Dihydroartemisinin: a potential drug for the treatment of malignancies and inflammatory diseases, Front. Oncol. 11 (October) (2021) 1–12, https://doi.org/10.3389/fonc.2021.722331.

[10] S. Dama, et al., A randomized trial of dihydroartemisinin-piperaquine versus artemether-lumefantrine for treatment of uncomplicated Plasmodium falciparum malaria in Mali, Malar. J. 17 (1) (2018), https://doi.org/10.1186/s12936-018-2496-x.

[11] J.D. Steyn, et al., Absorption of the novel artemisinin derivatives artemisone and artemiside: potential application of Pheroid™ technology, Int. J. Pharm. 414 (1–2) (2011) 260–266, https://doi.org/10.1016/j.ijpharm.2011.05.003.

[12] S.B. Lim, A. Banerjee, H. Önyüksel, Improvement of drug safety by the use of lipid-based nanocarriers, J. Control. Release 163 (1) (2012) 34–45, https://doi.org/10.1016/j.jconrel.2012.06.002.

[13] L. Zhang, S. Wang, M. Zhang, J. Sun, Nanocarriers for oral drug delivery, J. Drug Target. 21 (6) (2013) 515–527, https://doi.org/10.3109/1061186X.2013.789033.

[14] K.K. Singh, S.K. Vingkar, Formulation, antimalarial activity and biodistribution of oral lipid nanoemulsion of primaquine, Int. J. Pharm. 347 (1–2) (2008) 136–143, https://doi.org/10.1016/j.ijpharm.2007.06.035.

[15] P. Melariri, et al., Oral lipid-based nanoformulation of tafenoquine enhanced bioavailability and blood stage antimalarial efficacy and led to a reduction in human red blood cell loss in mice, Int. J. Nanomed. 10 (March) (2015) 1493–1503, https://doi.org/10.2147/IJN.S76317.

[16] S.E. Haas, C.C. Bettoni, L.K. de Oliveira, S.S. Guterres, T. Dalla Costa, Nanoencapsulation increases quinine antimalarial efficacy against Plasmodium berghei in vivo, Int. J. Antimicrob. Agents 34 (2) (2009) 156–161, https://doi.org/10.1016/j.ijantimicag.2009.02.024.

[17] N.G. Tayade, M.S. Nagarsenker, Development and evaluation of artemether parenteral microemulsion tayade and nagarsenker: artemether parenteral microemulsion, Indian J. Pharmaceut. Sci. 72 (5) (2010) 637–640 [Online]. Available: www.ijpsonline.com.

[18] J.O. Muga, J.W. Gathirwa, M. Tukulula, W.G.Z.O. Jura, In vitro evaluation of chloroquine - loaded and heparin surface - functionalized solid lipid nanoparticles, Malar. J. (2018) 1, https://doi.org/10.1186/s12936-018-2302-9. –7.

[19] X. Fernàndez-Busquets, Heparin-functionalized nanocapsules: enabling targeted delivery of antimalarial drugs, Future Med. Chem. 5 (7) (2013) 737–739, https://doi.org/10.4155/fmc.13.53.

[20] M.J. Boyle, J.S. Richards, P.R. Gilson, W. Chai, J.G. Beeson, Interactions with heparin-like molecules during erythrocyte invasion by Plasmodium falciparum merozoites, Blood 115 (22) (2010) 4559–4568, https://doi.org/10.1182/blood-2009-09-243725.

[21] M.F. Bastos, et al., Fucosylated chondroitin sulfate inhibits Plasmodium falciparum cytoadhesion and merozoite invasion, Antimicrob. Agents Chemother. 58 (4) (2014) 1862–1871, https://doi.org/10.1128/AAC.00686-13.

[22] R.G. Strickley, Solubilizing excipients used in commercially available oral and injectable formulations, Pharm. Res. (N. Y.) 21 (2) (2004) 201–230.

[23] C. Otuu, E.C. Ibezim, F. Kenechukwu, D. Odimegwu, "African journal of pharmaceutical,", Ajopred.Com 10 (January) (2011) 22–31 [Online]. Available: http://ajopred.com/wp-content/uploads/2015/04/Prevalence-of-Malaria-Among-Symptomatic-Children-Presumptively-Treated-with-Anti-Malarial-Medications-in-Edo-State-Nigeria.pdf.

[24] P. Prabhu, S. Suryavanshi, S. Pathak, S. Sharma, V. Patravale, Artemether–lumefantrine nanostructured lipid carriers for oral malaria therapy: enhanced efficacy at reduced dose and dosing frequency, Int. J. Pharm. 511 (1) (2016) 473–487, https://doi.org/10.1016/j.ijpharm.2016.07.021.

[25] J. Xu, et al., Wild Anopheles funestus mosquito genotypes are permissive for infection with the rodent malaria parasite, plasmodium berghei, PLoS One 8 (4) (2013) 8–11, https://doi.org/10.1371/journal.pone.0061181.

[26] P. Misra, N.L. Pal, P.Y. Guru, J.C. Katiyar, J.S. Tandon, Antimalarial activity of traditional plants against erythrocytic stages of plasmodium berghei, Pharm. Biol. 29 (1) (1991) 19–23, https://doi.org/10.3109/13880209109082843.

[27] M.K. Laryea, L.S. Borquaye, Antimalarial efficacy and toxicological assessment of extracts of some Ghanaian medicinal plants, J. Parasitol. Res. 2019 (2019), https://doi.org/10.1155/2019/1630405.

[28] A.S. Bassey, J.E. Okokon, E.I. Etim, F.U. Umoh, E. Bassey, Evaluation of the in vivo antimalarial activity of ethanolic leaf and stembark extracts of Anthocleista djalonensis, Indian J. Pharmacol. 41 (6) (2009) 258–261, https://doi.org/10.4103/0253-7613.59924.

[29] ICH Q1A(R2), International conference on harmonization (ICH). Guidance for industry: q1a(R2) stability testing of new drug substances and products, Ich Harmon. Tripart. Guidel. 4 (February) (2003) 24.

[30] Y. Gao, et al., In vitro release kinetics of antituberculosis drugs from nanoparticles assessed using a modified dissolution apparatus, BioMed Res. Int. 2013 (2013), https://doi.org/10.1155/2013/136590.

[31] S.V. Kumar, S.P. Kumar, D. Rupesh, K. Nitin, Journal of chemical and pharmaceutical research preparations, J. Chem. Pharm. Res. 3 (1) (2011) 675–684.

[32] V. Thiruvengadam, A.V. Bansod, Characterization of silver nanoparticles synthesized using chemical method and its antibacterial property, Biointerface Res. Appl. Chem. 10 (6) (2020) 7257–7264, https://doi.org/10.33263/BRIAC106.72577264.

[33] L. Tona, et al., " In-vivo antimalarial activity of Cassia occidentalism Morinda morindoides and Phyllanthus niruri ,", Ann. Trop. Med. Parasitol. 95 (1) (2001) 47–57, https://doi.org/10.1080/00034983.2001.11813614.

[34] E.R. Christensen, Dose-response functions in aquatic toxicity testing and the Weibull model, Water Res. 18 (2) (1984) 213–221, https://doi.org/10.1016/0043-1354(84)90071-X.

[35] I.J. Makowska, L. Vickers, J. Mancell, D.M. Weary, Evaluating methods of gas euthanasia for laboratory mice, Appl. Anim. Behav. Sci. 121 (3–4) (2009) 230–235, https://doi.org/10.1016/j.applanim.2009.10.001.

[36] X. Zhang, et al., Distribution and biocompatibility studies of graphene oxide in mice after intravenous administration, Carbon N. Y. 49 (3) (2011) 986–995, https://doi.org/10.1016/j.carbon.2010.11.005.

[37] G. Silva-Santana, et al., Clinical hematological and biochemical parameters in Swiss, BALB/c, C57BL/6 and B6D2F1 Mus musculus, Anim. Model. Exp. Med. 3 (4) (2020) 304–315, https://doi.org/10.1002/ame2.12139.

[38] X. Zhang, et al., Formulation optimization of dihydroartemisinin nanostructured lipid carrier using response surface methodology, Powder Technol. 197 (1–2) (2010) 120–128, https://doi.org/10.1016/j.powtec.2009.09.004.

[39] S. Dash, P.N. Murthy, L. Nath, P. Chowdhury, Kinetic modeling on drug release from controlled drug delivery systems, Acta Pol. Pharm. - Drug Res. 67 (3) (2010) 217–223.

[40] I. Permanadewi, A.C. Kumoro, D.H. Wardhani, N. Aryanti, Modelling of controlled drug release in gastrointestinal tract simulation, J. Phys. Conf. Ser. 1295 (1) (2019), https://doi.org/10.1088/1742-6596/1295/1/012063.

[41] F. Haghiralsadat, et al., A comprehensive mathematical model of drug release kinetics from nano-liposomes, derived from optimization studies of cationic PEGylated liposomal doxorubicin formulations for drug-gene delivery, Artif. Cells, Nanomedicine Biotechnol. 46 (1) (2018) 169–177, https://doi.org/10.1080/21691401.2017.1304403.

[42] A. Jain, S.K. Jain, In vitro release kinetics model fitting of liposomes: an insight, Chem. Phys. Lipids 201 (2016) 28–40, https://doi.org/10.1016/j.chemphyslip.2016.10.005.

[43] I.Y. Wu, S. Bala, N. Škalko-Basnet, M.P. di Cagno, Interpreting non-linear drug diffusion data: utilizing Korsmeyer-Peppas model to study drug release from liposomes, Eur. J. Pharm. Sci. 138 (June) (2019) 105026, https://doi.org/10.1016/j.ejps.2019.105026.

[44] Z. Yang, H. Peng, W. Wang, T. Liu, Crystallization behavior of poly(ε-caprolactone)/layered double hydroxide nanocomposites, J. Appl. Polym. Sci. 116 (5) (2010) 2658–2667, 10.1002/app.

[45] D.S. Villarreal-Lucio, J.L.R. Armenta, I.A.E. Moreno, R. Garcia-Alamilla, Effect of surfactant in particle shape and thermal degradation of eggshell particles, Mater. Res. 22 (3) (2019), https://doi.org/10.1590/1980-5373-MR-2018-0778.

[46] M.F. Queiroz, K.R.T. Melo, D.A. Sabry, G.L. Sassaki, H.A.O. Rocha, Does the use of chitosan contribute to oxalate kidney stone formation? Mar. Drugs 13 (1) (2015) 141–158, https://doi.org/10.3390/md13010141.

[47] C. Song, H. Yu, M. Zhang, Y. Yang, G. Zhang, Physicochemical properties and antioxidant activity of chitosan from the blowfly Chrysomya megacephala larvae, Int. J. Biol. Macromol. 60 (2013) 347–354, https://doi.org/10.1016/j.ijbiomac.2013.05.039.

[48] S. Jain, S.K. Jain, P. Khare, A. Gulbake, D. Bansal, S.K. Jain, Design and development of solid lipid nanoparticles for topical delivery of an anti-fungal agent, Drug Deliv. 17 (6) (2010) 443–451, https://doi.org/10.3109/10717544.2010.483252.

[49] E. Rostami, S. Kashanian, M. Askari, The effect of ultrasound wave on levothyroxine release from Chitosan nanoparticles, Adv. Mater. Res. 829 (November) (2014) 284–288, https://doi.org/10.4028/www.scientific.net/AMR.829.284.
[50] W.N. Omwoyo, et al., Preparation, characterization, and optimization of primaquine-loaded solid lipid nanoparticles, Int. J. Nanomed. 9 (1) (2014) 3865–3874, https://doi.org/10.2147/IJN.S62630.
[51] R.C. Huxford, K.E. Dekrafft, W.S. Boyle, D. Liu, W. Lin, Lipid-coated nanoscale coordination polymers for targeted delivery of antifolates to cancer cells, Chem. Sci. 3 (1) (2012) 198–204, https://doi.org/10.1039/c1sc00499a.
[52] Y. Liu, G. Yang, S. Jin, L. Xu, C.X. Zhao, Development of high-drug-loading nanoparticles, Chempluschem 85 (9) (2020) 2143–2157, https://doi.org/10.1002/cplu.202000496.
[53] W.N. Omwoyo, et al., Development, characterization and antimalarial efficacy of dihydroartemisinin loaded solid lipid nanoparticles, Nanomedicine Nanotechnology, Biol. Med. 12 (3) (2016) 801–809, https://doi.org/10.1016/j.nano.2015.11.017.
[54] A.R. Dudhani, S.L. Kosaraju, Bioadhesive chitosan nanoparticles: preparation and characterization, Carbohydr. Polym. 81 (2) (2010) 243–251, https://doi.org/10.1016/j.carbpol.2010.02.026.
[55] S.U. Rahman, S. Bilal, A.U.H. Ali Shah, Synthesis and characterization of polyaniline-chitosan patches with enhanced stability in physiological conditions, Polymers 12 (12) (2020) 1–13, https://doi.org/10.3390/polym12122870.
[56] D. Angeletti, T. Sandalova, M. Wahlgren, A. Achour, Binding of subdomains 1/2 of PfEMP1-DBL1 α to Heparan sulfate or heparin mediates Plasmodium falciparum rosetting, PLoS One 10 (3) (2015) 1–15, https://doi.org/10.1371/journal.pone.0118898.
[57] C.W. Fennell, et al., Assessing African medicinal plants for efficacy and safety : pharmacological screening and toxicology 94 (2004) 205–217, https://doi.org/10.1016/j.jep.2004.05.012.
[58] P. Nath, A. Yadav, Acute and sub-acute oral toxicity assessment of the methanolic extract from leaves of Hibiscus rosa-sinensis L. in mice, J. Intercult. Ethnopharmacol. 4 (1) (2015) 70, https://doi.org/10.5455/jice.20141028021746.
[59] S. Samat, N.A. Nor, F.N. Hussein, W. Iryani, W. Ismail, Effects of Gelam and Acacia Honey Acute Administration on Some Biochemical Parameters of Sprague Dawley Rats, 2014.
[60] N. Andr, E. Marianne, N. Lincopan, S. Duarte, E. Aparecida, "Acute , subacute toxicity and genotoxic effect of a hydroethanolic extract of the cashew, Anacardium occidentale L .)," 110 (2007) 30–38, https://doi.org/10.1016/j.jep.2006.08.033.